Supporting Information for

Evolutionary rescue and reintroduction of resistant frogs allows recovery in the presence of a lethal fungal disease

Roland A. Knapp, Mark Q. Wilber, Allison Q. Byrne, Maxwell B. Joseph, Thomas C. Smith, Andrew P. Rothstein, Robert L. Grasso, Erica Bree Rosenblum

Corresponding Author name. Roland A. Knapp
E-mail: roland.knapp@ucsb.edu

This PDF file includes:

Supporting text
Figs. S1 to S8
Tables S1 to S2
Legends for Dataset S1 to S4
SI References

Other supporting materials for this manuscript include the following:

Datasets S1 to S4

Supporting Information Text

1. Frog evolution in response to Bd

A. Methods. We compared frog genomes sampled in naive versus recovering populations. Bd-exposure histories of these populations are based on a decade or more of data from visual encounter surveys and Bd surveillance using skin swabbing (e.g., 1). Comparing populations with different infection histories allowed larger sample sizes and replication across the landscape. The alternative approach of comparing samples from the same populations before and after Bd exposure isn't feasible in this system because Bd arrived in most MYL frog populations decades ago and population persistence/recovery is rare and unpredictable. As a result, samples from recovering populations collected from before and after Bd exposure are not available and are unlikely to be available in the future.

B. Results. In the Results section of the main paper, we describe the stringent set of outlier SNPS (identified using a Bonferroni-corrected p-value of 0.01). The liberal set, identified using a Bonferroni-corrected p-value of 0.05, included 38 outliers (35 SNPs and 3 INDELS) from 30 distinct genes across 16 contigs. Our analysis found no significantly over-represented GO terms in this set of 30 genes, or in the set of 38 outlier regions identified with the splined window analysis.

In the comparison of individual outlier variants between naive and recovering populations, we detected consistent allele frequency changes across all genetic clusters for 1 of 7 of the associated genes (RIN3; Fig. 1). Nonetheless, for the other 6 genes we still found a statistically significant signal of selection in 2 of the 3 genetic clusters (containing populations 6, 7, 8, and 9; Fig. 1, Figure S1 A SI). Therefore, although some outlier variant associations have a more limited geographic extent than RIN3, they still describe parallel evolutionary changes following Bd exposure and are therefore interesting candidates for future studies.

2. Frog population recovery

A. Methods. Swab extracts were analyzed singly instead of in triplicate (2). For analysis of swabs collected during 2005–2014, we used standards developed from known concentrations of zoospores (3), and after 2014, we used standards based on single ITS1 PCR amplicons (4). Based on paired comparisons between samples analyzed using both types of standards, Bd in the study area has an average of 60 ITS1 copies per zoospore. To express all qPCR results as the number of ITS1 copies, starting quantities obtained using the zoospore standard (measured as "zoospore equivalents") were multiplied by 60. In addition, all qPCR quantities (regardless of standard) were multiplied by 80 to account for the fact that DNA extracts from swabs were diluted 80-fold during extraction and PCR (5).

3. Population viability modeling

A. Methods.

Incorporating yearly variability in vital rates We extracted yearly survival probabilities for translocated adults σ_{A_T} and naturally recruited adults σ_{A_R} from the CMR model used to estimate population-level parameters of translocated populations (see "Estimation of adult survival and population size" above). Although we observed yearly variability in adult survival within a population, the magnitude of this variability was small compared to among population variability (Fig. 3). Thus, we did not include yearly within-population variability in adult survival in this analysis. However, within a population there was substantial yearly variability in the successful recruitment of adults, greater than what we would expect from Poisson variability around a mean value. Therefore, we allowed for yearly variability in the probability of successful recruitment ω (additional details provided in "Estimating model parameters" below).

Estimating model parameters The baseline parameter values for the model and how they were estimated are given in Table S2 : SI. Parameters σ_{A_T} and σ_{A_R} were extracted directly from our CMR model described previously in this study. For populations where we had a sufficient number of PIT-tagged, naturally-recruited adults, we observed that σ_{A_T} and σ_{A_R} could be notably different, with $\sigma_{A_R} > \sigma_{A_T}$ (Figure S7 : SI). For populations lacking sufficient numbers of naturally-recruited adults, we were unable to directly estimate σ_{A_R}, and instead set $\sigma_{A_R} = \sigma_{A_T}$.

Model analysis and simulation We performed four analyses on our model. First, we considered a deterministic version of our model with no yearly heterogeneity in probability of successful recruitment ω, and calculated the predicted long-run growth rate λ of a population for different values of σ_{A_R} and ω. We then fixed $\omega = 0.3$ and calculated the predicted growth rate of our 12 populations.

Second, we performed a local elasticity analysis on λ with respect to parameters ω, σ_{A_R}, and F to determine how small changes in these parameters could influence the long-run deterministic growth rate of populations (Figure S8).

Third, we defined a version of the model with demographic and environmental stochasticity, where environmental stochasticity was represented by among-year variability in ω. We used this model to simulate a one-time introduction of 40 translocated adult frogs. We ran this simulation 1000 times for each population and computed the probability of a population becoming extinct after 50 years given the observed parameter values and environmental stochasticity in ω. We varied the mean recruitment

probability ω from 0.15 and 0.4 and drew values of ω each year from a beta distribution with a dispersion parameter of $\phi = 2$ (when $\omega = 0.5$ and $\phi = 2$ the beta distribution is uniform between 0 and 1).

Finally, we assessed whether our stochastic model could reproduce observed trajectories of population recovery. We focused on population 70550 because this was our longest CMR time series for a translocated population and because this population shows evidence of substantial post-translocation increases in adult abundance associated with population establishment and recovery. We simulated our model for 16 years, repeating the simulation 50,000 times. For each run and each year, we drew ω from a uniform distribution between 0 and 1 (or equivalently a beta distribution with mean 0.5 and $\phi = 2$). Using Approximate Bayesian Computing and rejection sampling (6), we identified the top 2% of trajectories (i.e., 1000 trajectories) that minimized the sum of squared errors between the observed and predicted data. The ω values associated with these "best" trajectories represented an approximate posterior distribution (7). Using these best fit trajectories, we assessed whether our model could qualitatively describe the patterns of recovery in the observed data for population 70550. Code to replicate the analyses can be found at https://github.com/SNARL1/translocation.

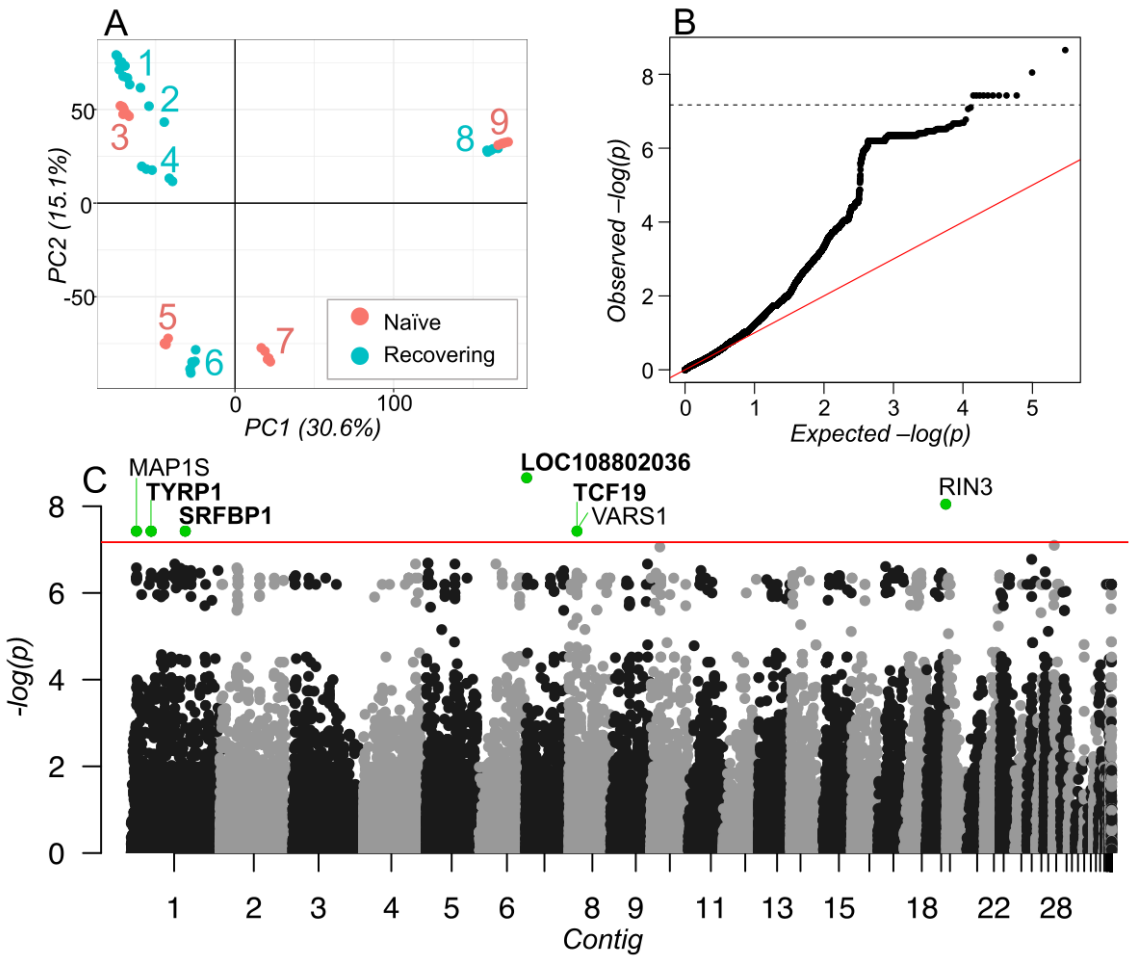

Fig. S1. Evidence for selection of individual variants in recovering MYL frog populations. (A) PCA calculated from binary SNPs showing the genomic relationship of samples. Numeric labels and colors match those in Fig. 1 A. (B) qqplot showing observed and expected p-values for 148,307 SNPs and INDELS as calculated in GEMMA. Dashed line shows p-value that identifies outliers. (C) Manhattan plot showing p-values for each SNP as calculated by GEMMA. SNPs are sorted by genomic position and contigs are sorted by size. Red line shows p-value that identifies outliers. Outlier SNPs above this threshold are highlighted and labeled. Bold labels indicate at least one non-synonymous SNP is present in that gene.

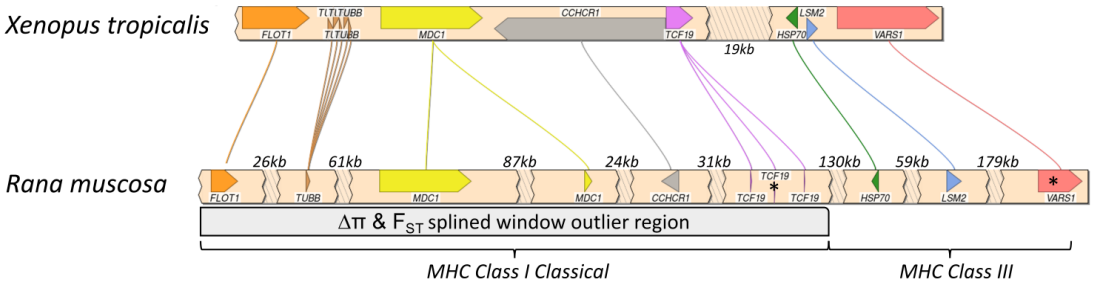

Fig. S2. Synteny plot showing conserved gene order in *Xenopus tropicalis* and *Rana mucosa* for the outlier region containing MHC Class I Classical and MHC Class III gene regions. The plot was created with SimpleSynteny (8) using *Xenopus tropicalis* Chromosome 8 (NC_030684.2, genbank accession GCA_000004195.4) and *Rana mucosa* Contig19. Astericks indicate the location of SNP outliers in TCF19 and VARS1 genes. Gap sizes for each contig representation are labeled.

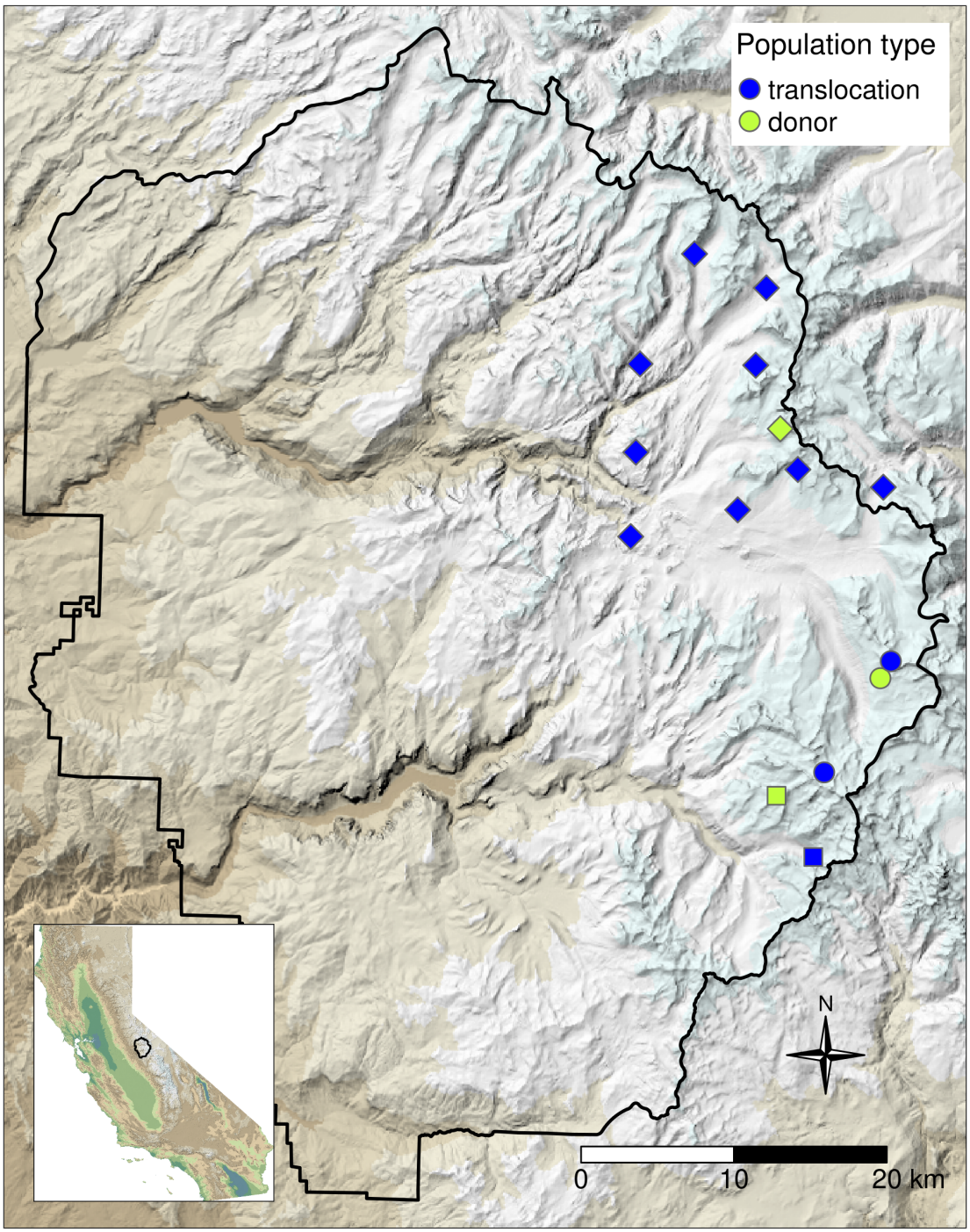

Fig. S3. Map showing the locations of translocated and donor MYL frog populations in Yosemite National Park (park boundary indicated by black polygon). Symbol shapes indicate the donor population used for each translocation site. To obscure the exact locations of populations, random noise was added to all point coordinates. Inset map shows the location of Yosemite within California. In both maps, elevation is indicated by the colored hillshade layer (dark green = lowest elevation, white = highest elevation).

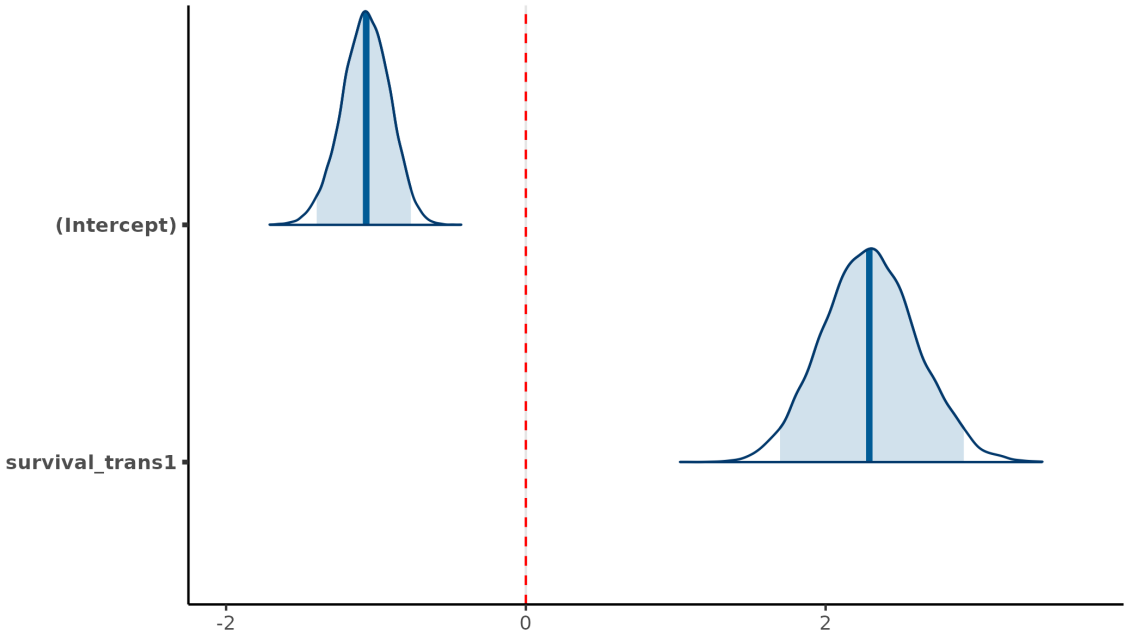

Fig. S4. For the best model describing the average 1-year survival of frogs in the first translocation to a site as a predictor of survival of frogs in all subsequent translocations to that site, estimated posterior density curves and shaded 95% uncertainty intervals for the intercept and single predictor variable. In the Bayesian framework in which the model was developed, a variable is considered an important predictor if the associated uncertainty interval does not overlap zero (indicated by the dashed red line).

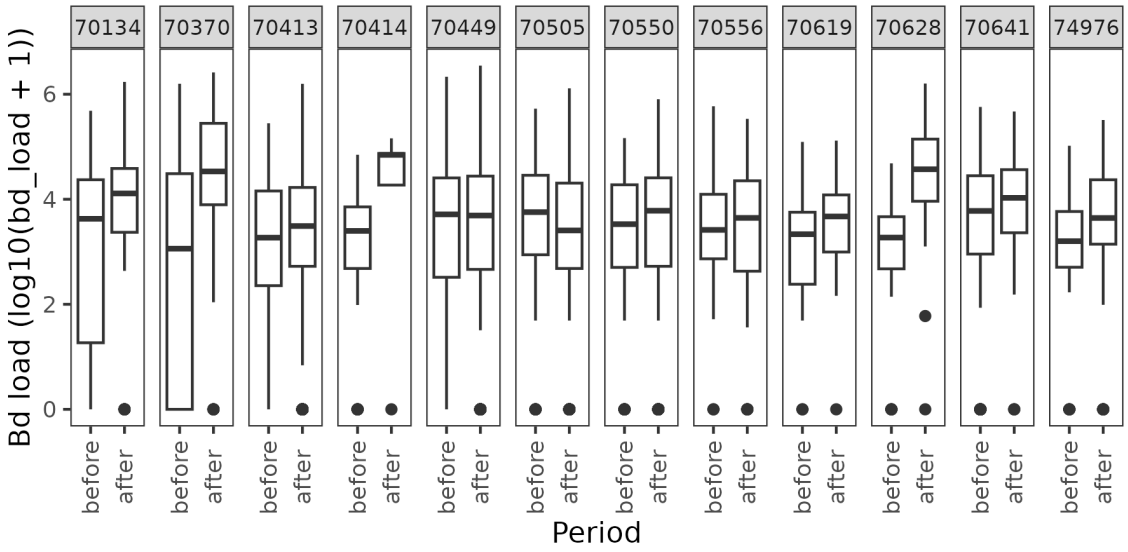

Fig. S5. Evidence that frogs translocated from recovering populations can maintain the benefits of resistance/tolerance in non-natal habitats. For frogs translocated to each of the 12 recipient sites, Bd loads for the period immediately prior to translocation versus during the 1-year period after translocation. Bd loads are expressed as the number of ITS1 copies per skin swab, as estimated by qPCR of the Bd ITS1 region. Loads indicative of severe disease are > 5.8 ITS copies (on a $\log_{10}$ scale; see SI text for details). Box plot details are as in Fig. 4.

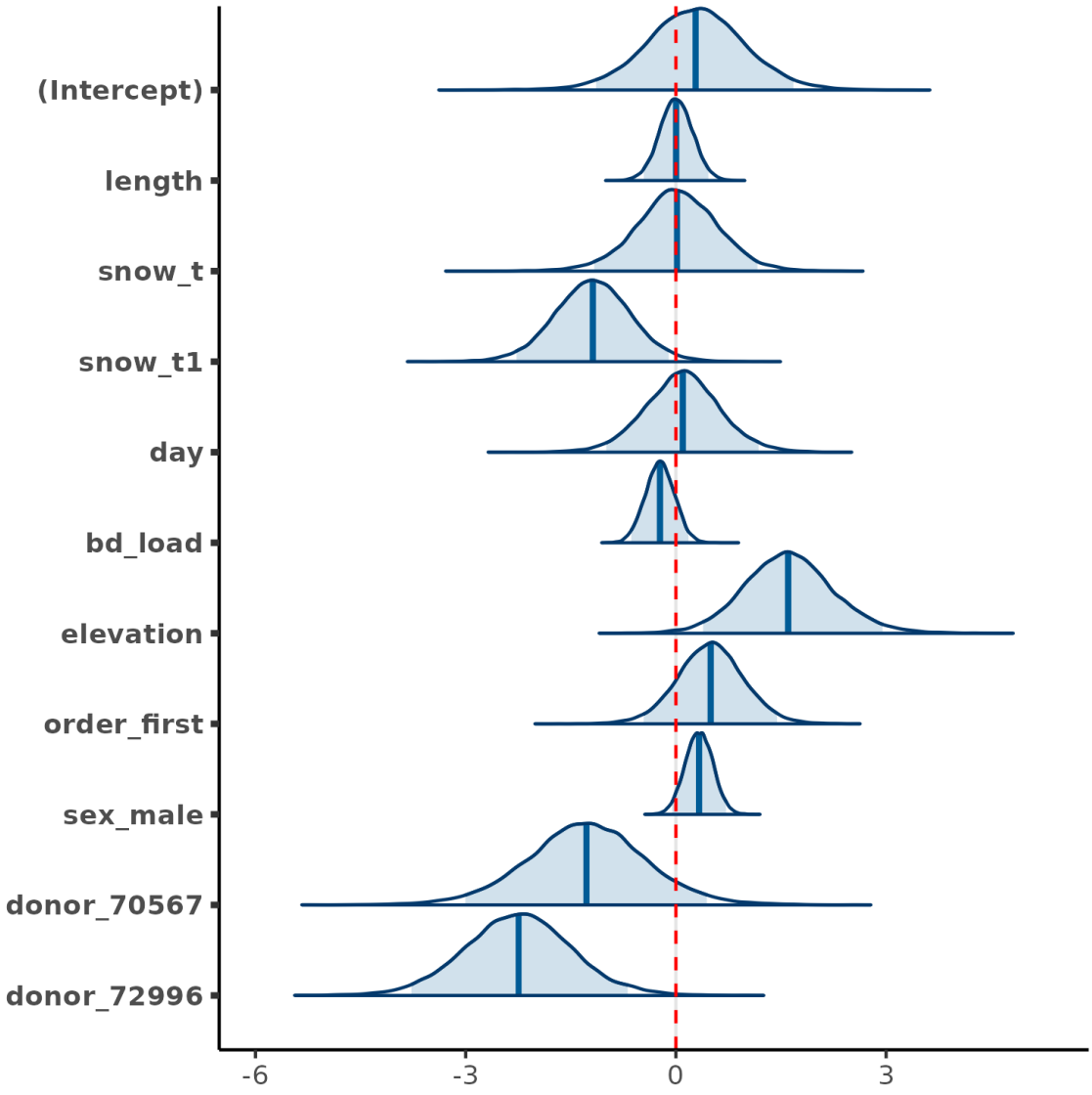

Fig. S6. Evidence that Bd load in not an important predictor of post-translocation frog survival. For the best model identifying predictors of 1-year frog survival following translocation, estimated posterior density curves and shaded 95% uncertainty intervals for the intercept and all predictor variables. In the Bayesian framework in which the model was developed, variables are considered important predictors if the associated uncertainty interval does not overlap zero (indicated by the dashed red line).

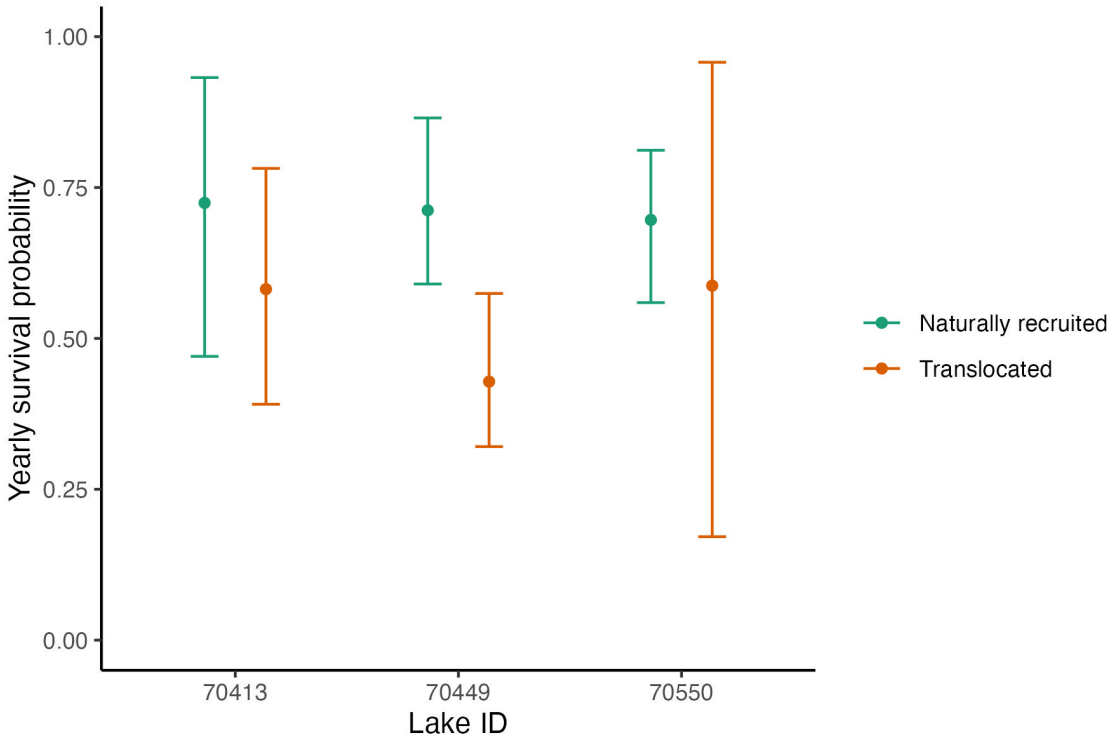

Fig. S7. Evidence that frog resistance/tolerance in non-natal habitats is maintained across generations. Comparison of the average yearly adult survival probabilities for adults translocated to each of three sites versus adults that were naturally recruited at each site (as a result of reproduction by translocated frogs). In contrast to Fig. 3, these are not survival probabilities from the first year following translocation, but instead represent averaged survival probabilities across multiple years and cohort. Points are median estimates and error bars give the 95% uncertainty intervals around the estimates, accounting for yearly variation in survival probabilities. The large error bars for 70550 reflect the large within and among individual variability in yearly survival probability at this site (as also reflected in one-year survival probabilities in Fig. 3). All estimates are derived from the mrmr package.

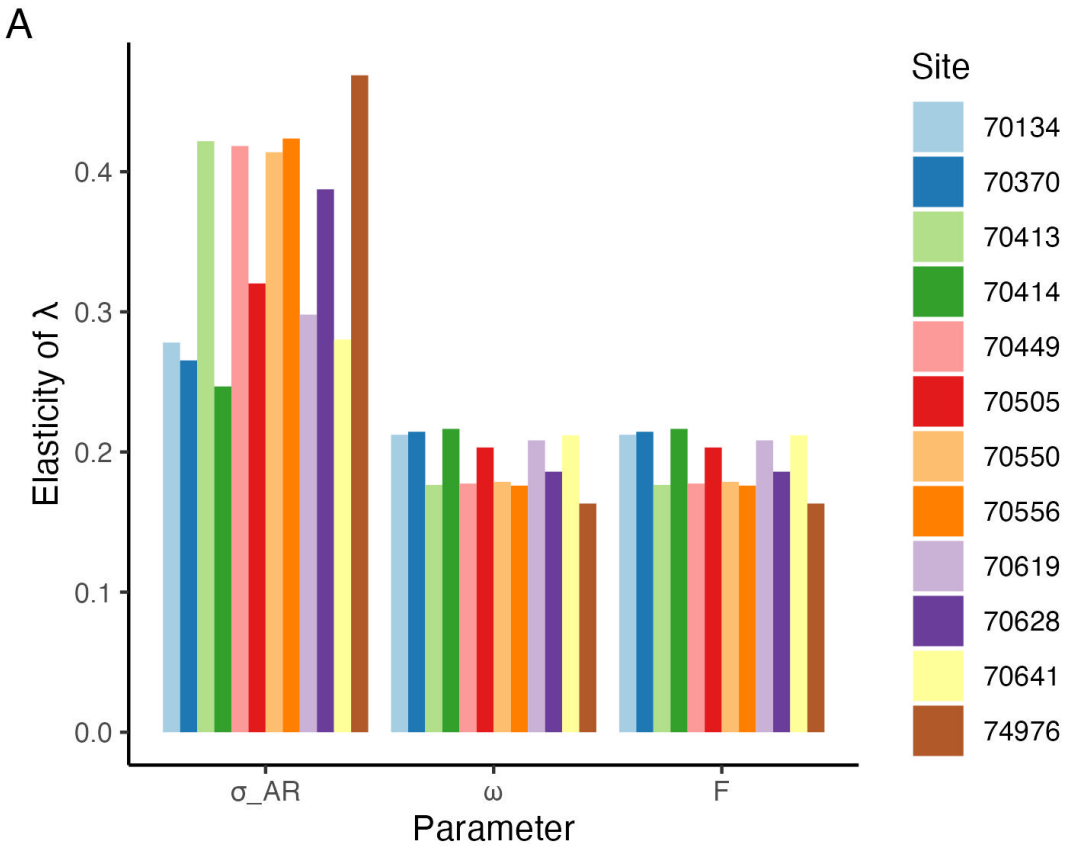

Fig. S8. Sensitivity analysis of the stage-structured MYL frog model. Elasticity of λ with changes in 3 parameters: σ_{A_R} (yearly survival probability of naturally recruited adults), ω (yearly probability of successful recruitment from juveniles to adults), and *F (*number of eggs produced by a female frog in a year that successfully hatch). Elasticity is calculated at the default parameter values for each population and ω = 0.3.

81 ***A.1. Tables.***

82

Table S1. Association between the proportion of populations translocated early versus late in the study period (< 2013 or >= 2013, respectively) and probability of survival (< 0.5 or >= 0.5). Based on the viability analysis, survival probabilities < 0.5 and >= 0.5 produced 50-year extinction probabilities of 1 and < 0.5, respectively.

Period	Survival probability	Number of translocations	Total translocations	Proportion of translocations
early	< 0.5	4	5	0.800
early	$>= 0.5$	1	5	0.200
late	< 0.5	2	7	0.286
late	$>= 0.5$	5	7	0.714

Table S2. Description and values of parameters used in the model. All survival probabilities are in the presence of the fungal pathogen Bd.

Parameter	Value	Source
σ_{L_1}, Yearly survival probability of year 1 tadpoles	0.7	Estimated from field data, observations, natural history knowledge
σ_{L_2}, Yearly survival probability of year 2 tadpoles	0.7	Estimated from field data, observations, natural history knowledge
σ_{L_3}, Yearly survival probability of year 3 tadpoles	0.7	Estimated from field data, observations, natural history knowledge
σ_{J_1}, Yearly survival probability of year 1 juveniles	0.25	Estimated from field data, observations, natural history knowledge
σ_{J_2}, Yearly survival probability of year 2 juveniles	0.5	Estimated from field data, observations, natural history knowledge
σ_{A_R}, Yearly survival probability of naturally recruited adults	Varies by population	Estimated from mark-recapture studies
σ_{A_T}, Yearly survival probability of translocated adults	Varies by population	Estimated from mark-recapture studies
p_{L_1}, Probability of a year 1 tadpoles remaining as a tadpoles	1	Estimated from field data, observations, natural history knowledge
p_{L_2}, Probability of a year 2 tadpoles remaining as a tadpoles	0.25	Estimated from field data, observations, natural history knowledge
p_{J_1}, Probability of a year 1 juvenile remaining as a juvenile	0.25	Estimated from field data, observations, natural history knowledge
p_F, Probability of a adult female reproducing in a year	0.5	Could be as high at 1, based on field observations
F, Number of surviving eggs produced by an adult female	100	From observations of captive frogs
ω, Probability of juvenile successfully recruiting to an adult	Varies yearly	Explored different values of this parameter

SI Dataset S1 (gemma_outliers_all.csv)
Set of liberal SNP and INDEL outlier variants (Bonferroni corrected p-value < 0.05), identified via GEMMA.

SI Dataset S2 (gemma_outliers_strict_freq.csv)
Set of strict SNP and INDEL outlier variants (Bonferroni corrected p-value < 0.01), identified via GEMMA. Additional information includes variant location within the gene (predicted_gene_loc) and whether the variant is synonymous or nonsynonymous (predicted_effect_AA).

SI Dataset S3 (spline_window_shared_outliers.csv)
Description of overlapping F_{ST} and π_{diff} outlier windows, as identified in the splined window analysis.

SI Dataset S4 (spline_window_gene_details.csv)
Annotation information for all genes within each of the overlapping outlier windows in dataset S3

References

1. RA Knapp, et al., Large-scale recovery of an endangered amphibian despite ongoing exposure to multiple stressors. *Proc. Natl. Acad. Sci. USA* **113**, 11889–11894 (2016).
2. K Kriger, J Hero, K Ashton, Cost efficiency in the detection of chytridiomycosis using PCR assay. *Dis. Aquatic Org.* **71**, 149–154 (2006).
3. D Boyle, D Boyle, V Olsen, J Morgan, A Hyatt, Rapid quantitative detection of chytridiomycosis (*Batrachochytrium dendrobatidis*) in amphibian samples using real-time Taqman PCR assay. *Dis. Aquatic Org.* **60**, 141–148 (2004).
4. AV Longo, et al., ITS1 copy number varies among *Batrachochytrium dendrobatidis* strains: implications for qPCR estimates of infection intensity from field-collected amphibian skin swabs. *PLoS ONE* **8**, e59499 (2013).
5. VT Vredenburg, RA Knapp, TS Tunstall, CJ Briggs, Dynamics of an emerging disease drive large-scale amphibian population extinctions. *Proc. Natl. Acad. Sci. USA* **107**, 9689–9694 (2010).
6. M Kosmala, et al., Estimating wildlife disease dynamics in complex systems using an Approximate Bayesian Computation framework. *Ecol. Appl.* **26**, 295–308 (2016).

7. MA Beaumont, Approximate Bayesian Computation in evolution and ecology. *Annu. Rev. Ecol. Evol. Syst.* **41**, 379–406 (2010).
8. D Veltri, MM Wight, JA Crouch, Simplesynteny: a web-based tool for visualization of microsynteny across multiple species. *Nucleic Acids Res.* **44**, W41–W45 (2016).